BA-92-2-2 #5856

ISOTHERMAL AIRFLOW CHARACTERISTICS IN A VENTILATED ROOM WITH A SLOT INLET OPENING

Y. Jin, Ph.D. **J.R. Ogilvie, Ph.D., P.Eng.**

ABSTRACT

The effect of inlet configuration on room air movement was investigated in a full-scale model in a comprehensive experiment. Room flow patterns were identified by zones and boundaries on an airflow rate plan. Velocities in the occupied zone were correlated well with the inlet parameters as long as airflow stayed in the full rotary flow zone on the plan. Regression equations, obtained through dimensional analysis and from the measurements at 41 inlet conditions, showed that the mean and turbulent fluctuations of flow velocity were nearly proportional to the incoming air speed at the slot inlet and to the opening height raised to the 0.6 power. Good correlations were also found between the velocity in the occupied region and the inlet jet momentum number.

INTRODUCTION

Air movement in the occupied zone is an important factor that directly affects the comfort and well-being of human occupants. Air movement is a complicated process that is a combined result of dynamic, thermal, and geometric influences. Understanding on this issue is still limited because each investigation can examine only a few influences and introduces certain assumptions and simplifications.

Mathematical and physical modeling are the two common methods of analysis of internal airflow characteristics. Most of the experimental studies have been performed in small-scale physical models to predict reality in full scale (Nielsen et al. 1978; Gosman et al. 1980; Timmons et al. 1980; Timmons 1984; Zhang et al. 1990). However, there are certain difficulties involved in physical model simulation. It seems to inevitably distort the similitude of dimensionless π terms between model and prototype for a general flow situation; therefore, a discrepancy may be introduced due to this technique. Increasing the flow velocity due to decreasing physical dimensions may significantly change the turbulent structure of the airflow, such as the spectral density distribution of the turbulent kinetic energy. Furthermore, some flow phenomena are very difficult or impossible to reproduce in reduced-size models. Therefore, except for the financial advantage, a test in the 1:1 scale remains essential to exactly reproduce the three-dimensional room flow (Moog 1981).

Among various mathematical models, the k-ε fully turbulent model appears promising with the advent of modern computers. The common k-ε model suffers from the condition of requiring fully turbulent flow. Nevertheless, most ventilation airflows encountered in residential and office buildings are not fully turbulent and break the basic assumption of the k-ε model. Recently, the fully turbulent k-ε model was modified by using empirically derived expressions and constants to account for the "low Reynolds number" effect (Lam and Bremherst 1981; Patel et al. 1985; Chen et al. 1990; Hoff et al. 1990). However, computations in the numerical simulation are very expensive. Some predicted results compared poorly with experimental measurements.

In this study, an attempt was made to experimentally determine airflow patterns and velocity distribution in a full-scale room with a continuous slotted inlet opening. Ventilation flow rates up to 60 air changes per hour (ach) were examined. Although such high flow rates are much above 15 ach—the highest rate for an occupied office building—they may provide information for other types of structures, such as those for industrial, agricultural, and other purposes. For example, Spitler et al. (1991) used up to 100 ach in a study of night purging strategy for a modeled office building.

HYPOTHESIS AND DIMENSIONAL ANALYSIS

Gosman et al. (1980) reported that the maximum velocity in the reverse flow is essentially determined by the area of the supply opening and not by its shape, and the result obtained from three-dimensional flow was only 10% to 30% lower than that from two-dimensional ones. To simplify the research, a slot opening immediately underneath the smooth ceiling (Figure 1) was used instead of square or rectangular inlets. With slot length extending to the full width of the room, the interior air movement was assumed to be two-dimensional. The flow was also isothermal and steady state. Room airflow characteristics are primarily influenced by the performance of the air supply opening (ASHRAE 1985). The inlet Reynolds number and the inlet jet momentum number are commonly used indices to determine the air speed in the occupied zone (Timmons et al. 1980; Timmons 1984; Ogilvie and Barber 1989; Spitler et al. 1991). In this study, it was postulated that

Yuzhou Jin, Ph.D., is a research associate and **John R. Ogilvie**, Ph.D., P.Eng., is a professor in the School of Engineering, University of Guelph, Ontario, Canada.

THIS PREPRINT IS FOR DISCUSSION PURPOSES ONLY, FOR INCLUSION IN ASHRAE TRANSACTIONS 1992, V. 98, Pt. 2. Not to be reprinted in whole or in part without written permission of the American Society of Heating, Refrigerating, and Air-Conditioning Engineers, Inc., 1791 Tullie Circle, NE, Atlanta, GA 30329. Opinions, findings, conclusions, or recommendations expressed in this paper are those of the author(s) and do not necessarily reflect the views of ASHRAE. Written questions and comments regarding this paper should be received at ASHRAE no later than July 8, 1992.

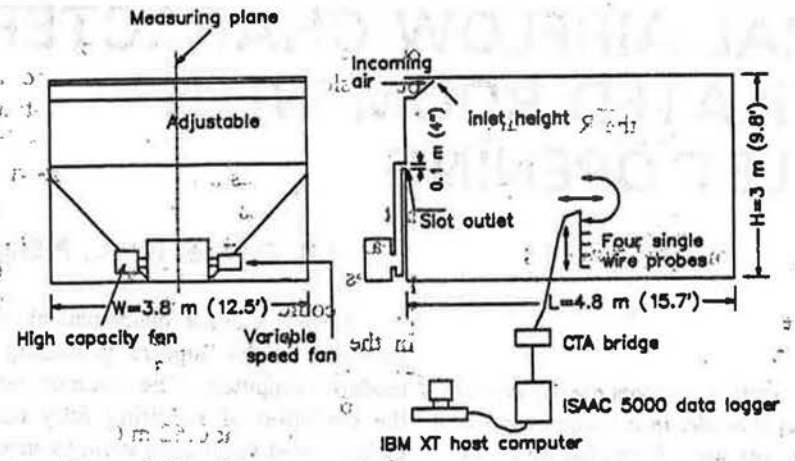

Figure 1 Dimensions and geometries of the experimental enclosure and apparatus.

room airflow patterns and air velocities in the occupied zone can be shown on an airflow rate plan in Cartesian coordinates with the incoming jet air speed at the inlet, U_0, as the x axis and the inlet opening height, d, as the y axis (Figure 2). Any point on this plan represents a ventilation rate through the inlet for a unit room width or an inlet Reynolds number. Based on the airflow rate plan, the following hypotheses were postulated.

1. Airflow rates expressed on an airflow rate plan can be divided into three zones according to different airflow characteristics in the floor region. In zone A, airflow in the occupied zone remains stagnant, or the mean air velocity within the area is less than 0.1 m/s (20 fpm). In zone C, the full rotary flow pattern is formed. The direction of air movement in the floor region is consistent with the rotating airflow along the room perimeter. Within zone B, which is an intermediate zone between zones A and C, the rotary flows are not formed, but the mean air velocity over the occupied zone is greater than 0.1 m/s (20 fpm).
2. The boundaries dividing the three zones (i.e., the stagnant, intermediate, and full rotary flow zones) are neither straight nor hyperbolic lines. A straight boundary line would indicate that there is a linear relationship between inlet air velocity and inlet height; hence, only one of them is an independent variable in the airflow rate or inlet Reynolds number. A hyperbolic boundary line indicates that the inlet air speed and the inlet height have an equal weight of influence on room air characteristics. Only the product of the two factors is the determinant, regardless of the magnitude of each.

   In zone C of the airflow rate plan, the airflow direction at the floor of the rotary flow is opposite to that at the ceiling, where the wall jet is created, i.e., the reverse flow of Nielsen et al. (1978) and Gosman et al. (1980). The mean and the root-mean-square (RMS) values of the velocity in the reverse flow are the most interesting parameters in this study and are referred to as dependent variables. The independent variables are U_0 and d. Other hypotheses about reverse flow velocity in the full rotary flow zone follow.
3. U_0 and d do not have equal influence on the reverse flow velocity. In other words, the velocity cannot be expressed solely by the ventilation flow rate through the inlet or the Reynolds number based on U_0 and d.
4. The mean velocity and the RMS value of the flow at the floor, normalized by the inlet velocity, are non-linearly proportional to the inlet height to room width ratio. Nevertheless, these dimensionless terms do not change with inlet Reynolds number.

A general equation describing air velocity in the reverse flow for a unit room width is

$$f_1(U, U_0, d, L, H, x, y, \rho, \mu, P) = 0 \qquad (1)$$

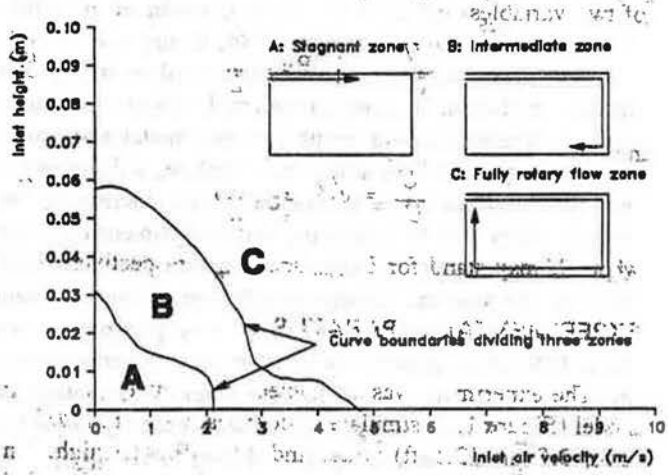

Figure 2 Postulated airflow rate plan.

where

U = floor mean air velocity, U_{mean} and the RMS value U_{rms}, respectively, m/s;
U_0 = inlet air velocity, m/s;
d = inlet slot height, m;
L = room length (in direction of initial flow), m;
H = room height, m;
x = horizontal coordinate, m;
y = vertical coordinate, m;
ρ = air density, kg/m^3;
μ = air viscosity, kg/(m·s); and
P = air pressure, Pa.

To simplify, air pressure inside the room is assumed to be the same everywhere. If an average velocity value is used, the local velocity at each x and y position does not appear in the expression. Then Equation 1 becomes

$$f_2(U, U_0, d, L, H, \rho, \mu) = 0, \quad (2)$$

which may be expressed by the dimensionless form

$$\frac{U}{U_0} = g_1(\mathrm{Re}_d, \frac{d}{L}, \frac{H}{L}) \quad (3)$$

where the inlet Reynolds number $\mathrm{Re}_d = (\rho U_0 d)/\mu$.

However, a change in d results in changes in Re_d and d/L simultaneously, which causes difficulty in experimental design. If L is a constant, the characteristic length scale, d, in Reynolds number may be replaced by L, i.e., $\mathrm{Re}_L = (\rho U_0 L)/\mu$, and the corresponding dimensionless equation is

$$\frac{U}{U_0} = g_2(\mathrm{Re}_L, \frac{d}{L}, \frac{H}{L}). \quad (4)$$

The results obtained by Equations 3 and 4 are the same.

For the present study, both L and H are constant. Equations 3 and 4 may be further simplified as the function of two variables,

$$\frac{U}{U_0} = g_1'(\mathrm{Re}_d, \frac{d}{L}) \quad (5)$$

and

$$\frac{U}{U_0} = g_2'(\mathrm{Re}_L, \frac{d}{L}) \quad (6)$$

where U may stand for U_{mean} and U_{rms}, respectively.

EXPERIMENTAL APPARATUS

The experiment was conducted in an empty prototype model (Figure 1) to simulate a room that is 4.8 m (15.7 ft) long, 3.8 m (12.5 ft) wide, and 3 m (9.8 ft) high. An adjustable slot inlet and 0.1-m (4-in.) slot outlet extended the full width of the room (3.8 m [12.5 ft]). Air was exhausted evenly across the exit plane through the slot outlet and then via a contraction section, which linked the outlet slot and the suction fans. Room ventilation rates up to 60 ach were achieved by adjusting a vent on the fan box, the speed of the fan, or a combination of the above.

Velocity was measured by hot-wire anemometry. Four hot-wire probes were mounted on a testing rig, each separated by 0.04 m (1.57 in.). The testing rig moved the probes in both horizontal and vertical directions so that the probes could reach any test point in the centerline section. In the floor region, measurements were taken every 0.2 room widths (0.96 m [3.2 ft]) horizontally and every 0.04 m (1.6 in.) vertically, with the first point at 0.02 m (0.8 in.) and the last at 0.62 m (2 ft) above the floor. A total of 80 points were measured for each inlet setting.

A separate hot-wire probe was mounted in the center of the inlet slot to determine the incoming jet air speed. The probe was positioned exactly at the plane of the opening; therefore, a discharge coefficient was not needed in the calculation. All data were sampled by a high-speed, analog-to-digital data logger controlled by a host computer. Flow visualization was realized by ejecting smoke through the inlet slot. A propane-heated smoke generator burning mineral oil produced white smoke. Air temperature was measured by a calibrated thermocouple at the inlet and immediately beside the probes on the testing rig at the floor.

Hot-wire probe calibration was achieved by two devices—a rotating device and a wind tunnel—for the calibration speed ranges from 0.1 to 1.0 m/s (20 to 200 fpm) and from 1.0 to 15 m/s (200 to 2,950 fpm), respectively. Any effect due to temperature difference between calibration and measurement was corrected. Details about hot-wire calibration are given in Jin (1991).

SAMPLING PARAMETERS OF AIRFLOW

To obtain full flow information, the sampling frequency of the hot-wire probe must be at least twice as high as the highest frequency in the flow, according to the Nyquist sampling theorem (Leigh 1985). Meanwhile, sampling time must be long enough to get a stable mean velocity from a turbulent flow. On the other hand, sampling frequency and sampling time should be as low as possible from the viewpoint of computer memory and computing time.

The sampling frequency was chosen as 100 Hz after determining that there was little loss of information compared to 1,600 Hz (Jin 1991). At this frequency, Figure 3 shows the mean and RMS of the velocity, and turbulence intensity changing with the length of sampling time up to 150 seconds. When the sampling time was longer than 30 seconds, the variation of mean velocity was within 0.05 m/s (10 fpm), RMS within 0.02 m/s (4 fpm), and turbulence intensity within 3%. These experimental errors are within the requirements of this study. Mean and RMS values obtained from these 3,000 data (100 Hz times 30 s) were used to evaluate the velocity characteristics for

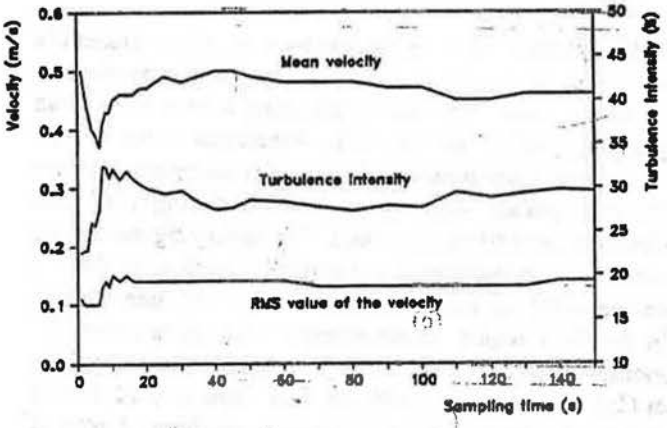

Figure 3 *The effect of the length of the sampling time at 100 Hz.*

a measuring position since the steady-state air velocity was close to a normal or Gaussian distribution (Jin 1991).

EXPERIMENTAL METHOD

To identify the three zones on a postulated airflow rate plan, 14 levels of inlet velocity and 10 levels of inlet height were selected as the inlet configurations (Table 1). Each combination of the levels is a possible point in the plan. More points were arranged for lower ventilation rates to get detailed information about certain areas. Sixty ach was considered the maximum ventilation rate; therefore, a hyperbolic line $U_0 d = 0.24$ m^3/(s·m) (155 ft^3/min·ft) on this plan marked the upper limit flow rate for the room with unit width (4.8 m [15.7 ft] long and 3 m [9.8 ft] high).

The boundary dividing zones A and B, i.e., the stagnant zone and intermediate zone, were determined by measuring the air velocity at the floor region for each inlet configuration. First, the inlet height was fixed and the inlet velocity was changed. If the mean velocity over the floor was less than 0.1 m/s (20 fpm), then this point in the airflow rate plan belonged to the stagnant zone (zone A). The inlet velocity was raised until the floor velocity was greater than 0.1 m/s (20 fpm). The boundary, therefore, was located between the two points. Then, the same procedure was repeated at another inlet height.

The boundary dividing zones B and C, i.e., between the intermediate zone and the rotating airflow zone, were determined by flow visualization. Smoke was injected for each inlet configuration, and internal flow patterns were observed. The boundary was located between those points just before and then after the full rotary flow pattern was formed.

To formulate the relationship between floor velocity and inlet configurations in zone C, velocity at the floor was measured for combinations of inlet levels that fell into zone C; these levels are marked with an asterisk (*) in Table 1. Because the relationships were only distinct in zone C, these measurements were not conducted until the three zones had been identified. Figure 4 shows the 35 combinations of U_0 and d between the lower boundary of rotary flow and the upper limit flow rate. Replication was conducted at six points with the same ventilation rates of 15 and 40 ach to test the effects of experimental error and flow rate.

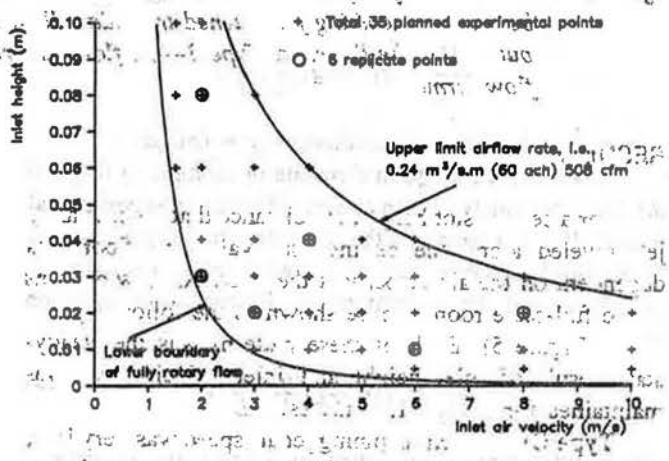

Figure 4 *Planned experimental and replication points between lower boundary of full rotary flow and upper limit flow rate on the airflow rate plan.*

TABLE 1
Inlet Configurations to Identify Three Zones and Formulate Equations in Zone C

Inlet Velocity U_0 (m/s)	0.5	1	1.5	2	2.5	3	3.5	4*	4.5	5*	5.5	6*	8*	10*
(fpm)		200		400		600		800		1000		1200	1600	2000
Inlet Height d (m)	.005*	.01*	.015	.02*	.025		.03*	.04*		.06*		.08*	.10*	
(in.)	.2	.4	.6	.8	1		1.2	1.6		2.4		3.2	4	

*Levels at which velocity was measured at 80 floor positions to establish relationships in zone C.

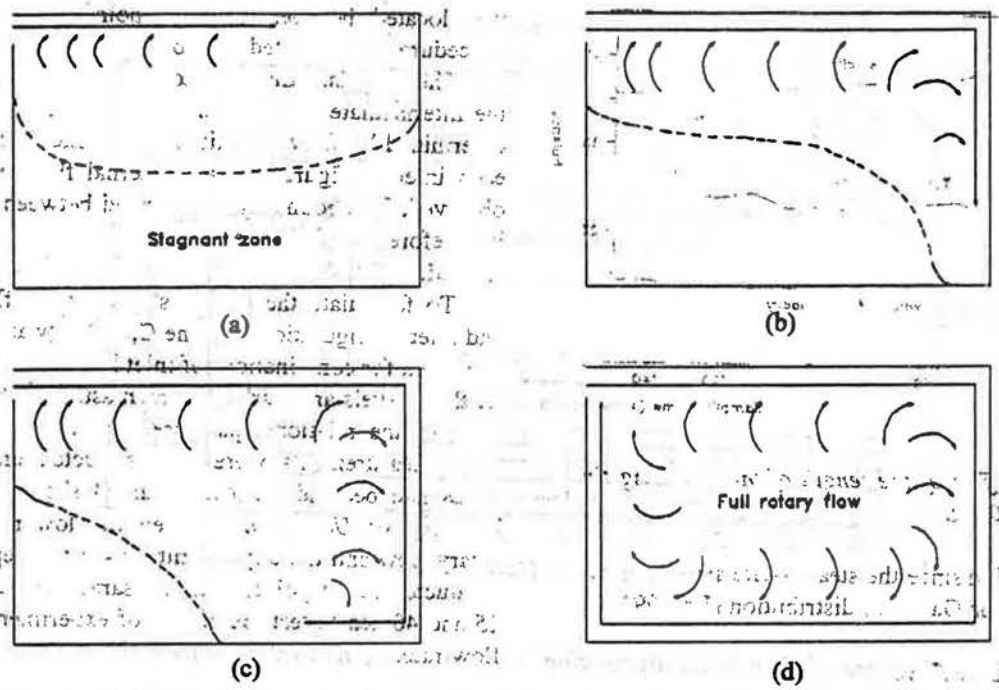

Figure 5 *Four types of airflow patterns visualized in a prototype slot-ventilated enclosure. (a) Type 1—the flow patterns before the incoming jet reached the sidewall. (b) Type 2—the flow patterns after the jet reached the sidewall but before the floor. (c) Type 3—the flow patterns after the jet reached the floor. (d) Type 4—the full rotary flow formed.*

RESULTS

For a certain slot height, the distance that the incoming jet traveled along the ceiling, sidewall, and floor was dependent on the air velocity at the inlet. Airflow patterns in the full-scale room can be shown as the following four types (Figure 5). Each of these patterns was the steady-state result of inlet height and inlet velocity and was maintained for at least 15 minutes.

Type One When incoming jet air speed was very low, the jet did not contain sufficient energy to reach the sidewall (Figure 5a). The solid line with the arrow represents the incoming jet air. The curved arrows represent the immediate surrounding air entrained by the jet. The dotted line outlines boundaries of the spreading region of the smoke. In the floor region, the mean air velocity was less than 0.1 m/s (20 fpm).

Type Two With a higher incoming air velocity, the jet air reached the sidewall and flowed along the wall toward the floor (Figure 5b). The spreading region of the smoke increased and included a part of the occupied zone near the corner. The mean velocity at the floor region was greater than 0.1 m/s (20 fpm).

Type Three If the inlet velocity was even higher, the jet air then reached the floor and traveled along the floor (Figure 5c). The entrainment of room air became more significant. The spreading smoke region included most of the room area. With time, the small space between the floor and the wall with the inlet was eventually filled up with smoke by convection and diffusion.

Type Four A further increase of inlet velocity resulted in the formation of full rotary flow (Figure 5d). Any further increase in the inlet velocity will not change the flow patterns but will increase the velocity in the rotary flow. Figure 6 shows a typical distribution of velocity along room surfaces when full rotary flow patterns have been reached.

The airflow was observed according to the levels listed in Table 1. To simplify, type one of the flow patterns was defined as a stagnant flow region at the floor (zone A) and type four was defined as full rotary flow (zone C). Any patterns between types one and four were referred to as the intermediate flow patterns (zone B). The results are shown on an airflow rate plan (Figure 7).

The zone boundaries were determined by the nonlinear least-squares method (SAS 1988). The expression of the boundary dividing the three zones is

$$dU_0^n = C_1. \tag{7}$$

With the inlet slot length equal to the room width, it can be expressed in terms of ventilation flow rate (ach) for the unit length of the room:

$$\frac{QU_0^{n-1}}{V} = C_2 \tag{8}$$

where

Q = volume flow rate through the inlet, m^3/s;
V = volume of the room, m^3; $V = L$ (4.8 m [15.7 ft]) · W (1 m [3.28 ft]) · H (3 m [9.8 ft]);

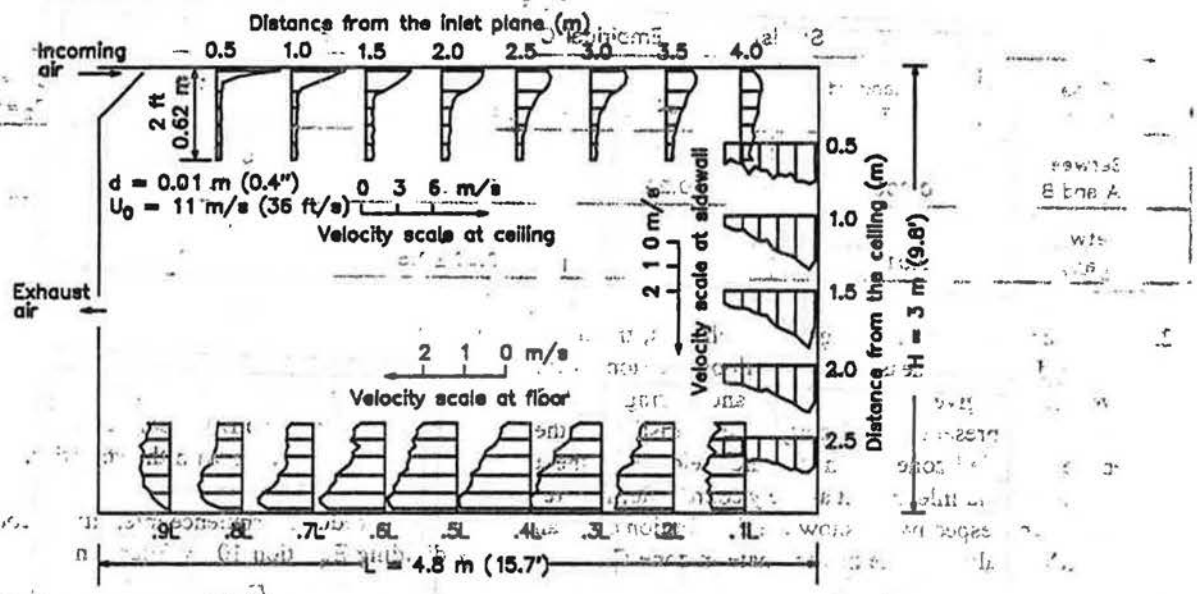

Figure 6 *Diagrams of air velocity distribution in the enclosure up to 0.62 m from the surfaces.*

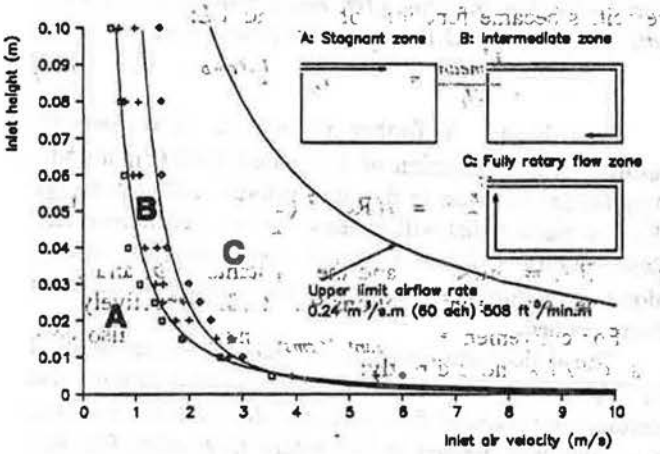

Figure 7 *Measured and regressed boundaries dividing the airflow rate plan into three zones that represent three types of flow patterns.*

n, C_1, and C_2 = empirical constants listed in Table 2 along with the statistics for the equations.

The floor velocity in zone C was processed in two ways:

1. For each of the 80 positions, the velocity was normalized by the inlet velocity and then averaged over 41 inlet settings, i.e., 35 inlet conditions plus six replicates (Figure 4), to get an overall view of the flow image at the floor. The distribution of mean velocity and RMS value is shown in Figures 8a and 8b, respectively.

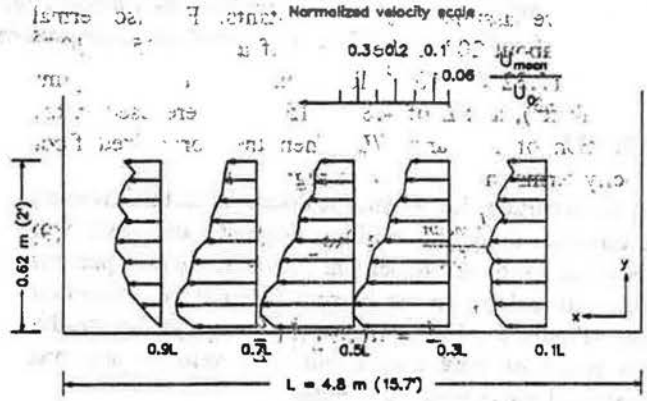

Figure 8a *The normalized mean velocity profiles at five horizontal positions along the floor averaged over 41 inlet conditions.*

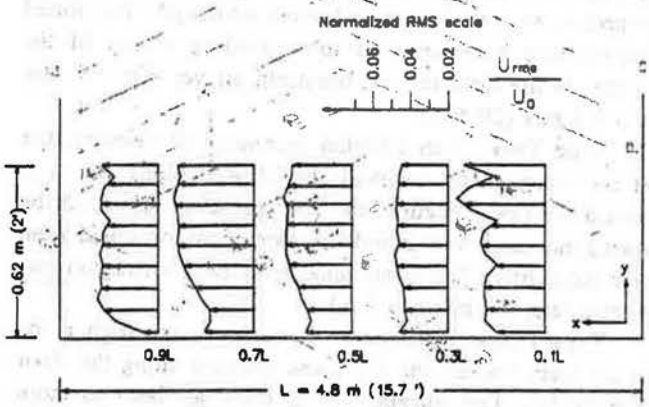

Figure 8b *The normalized profiles of RMS value at five horizontal positions along the floor averaged over 41 inlet conditions.*

TABLE 2
Statistics and Empirical Constants for Zone Boundaries

Zone Boundaries	Standard Error	R^2	Exponent n ± Std. Err.	Constant C_1 ± Std. Err.	Constant C_2 $C_2 = C_1/(WH)$
Between A and B	0.0037	0.99	1.65 ± 0.08	0.04589 ± 0.00149	0.0032
Between B and C	0.011	0.89	2.50 ± 0.51	0.1363 ± 0.0223	0.0095

2. For each of the inlet settings and replicates, the mean and RMS values measured at 80 floor positions were averaged to give a single mean and a single RMS value to represent the velocity characteristics in the entire occupied zone. With the inlet velocity as the x coordinate and inlet height as the y coordinate, Figures 9a and 9b, respectively, show the distribution of mean and RMS values as the z coordinate in zone C.

Experimental data processed by the second method were used to develop relationships suggested by the dimensional analysis. The dimensionless terms Re_L and d/L in Equation 6 are actually the scaled U_0 and d since L, μ, and ρ were assumed to be constants. For isothermal airflow at about 20°C, the values of μ of 1.815×10^{-5} kg/(m·s) (7.32×10^{-4} lb/ft·min), ρ of 1.15 kg/m^3 (0.072 lb/ft^3), and L of 4.8 m (15.7 ft) were used in the calculation of Re_L and d/L. Then the normalized floor velocity terms in zone C were regressed:

$$\frac{U_{mean}}{U_0} = a(Re_L)^b \left(\frac{d}{L}\right)^c , \qquad (9)$$

$$\frac{U_{rms}}{U_0} = a(Re_L)^b \left(\frac{d}{L}\right)^c , \qquad (10)$$

where

Re_L = $(\rho U_0 L)/\mu$, and
a, b, and c = empirical constants listed in Table 3 along with the statistics.

As a product, turbulence intensity, I, could be obtained by dividing Equation 10 by Equation 9:

$$I = \frac{U_{rms}}{U_{mean}} = a(Re_L)^b \left(\frac{d}{L}\right)^c . \qquad (11)$$

Constants a, b, and c are in Table 3.

By rearranging Equations 9 and 10, the dimensionless velocities became functions of Re_d and d/L:

$$\frac{U_{mean}}{U_0} = a(Re_d)^b \left(\frac{d}{L}\right)^{(c-b)} \qquad (12)$$

and

$$\frac{U_{rms}}{U_0} = a(Re_d)^b \left(\frac{d}{L}\right)^{(c-b)} \qquad (13)$$

where $Re_d = (\rho U_0 d)/\mu$, and the constants a, b, and c are the same as those in Equations 9 and 10, respectively.

For convenience, U_{mean}, U_{rms}, and I were also correlated to U_0 and d directly:

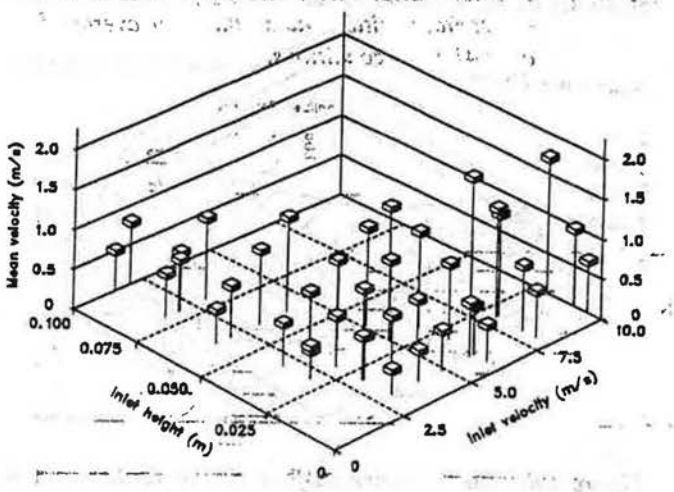

Figure 9a *Measured mean velocities at the floor for different combinations of inlet velocity and inlet height in the full rotary flow zone.*

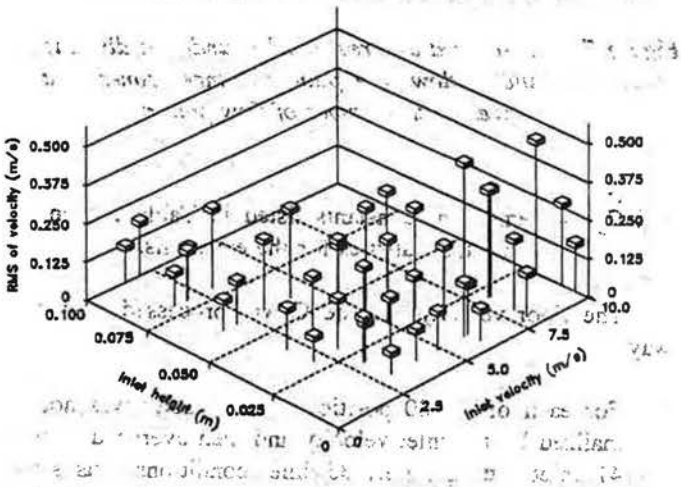

Figure 9b *Measured RMS values of velocity at the floor for different combinations of inlet velocity and inlet height in the full rotary flow zone.*

TABLE 3
Statistics and Empirical Constants for Equations

Dependent Variables	Equation Number	Standard Error	R^2	Intercept $a \pm$ Std. Err.	Exponent $b \pm$ Std. Err.	Exponent $c \pm$ Std. Err.
$\frac{U_{mean}}{U_0}$	9	.014	.98	2.545 ± .773	.029 ± .027	.58 ± .02
$\frac{U_{rms}}{U_0}$	10	.0044	.96	.1479 ± .0570	.13 ± .03	.58 ± .03
I	11			.05805	.10	-.004
U_{mean}	14	.049	.98	1.568 ± .075	1.04 ± .02	.61 ± .02
U_{rms}	15	.0016	.97	.3608 ± .0219	1.09 ± .03	.60 ± .02
I	16	.017	.34	.2356 ± .0115	.10 ± .03	.021 ± .018

$$U_{mean} = a\,U_0^{\,b}\,d^{c}, \tag{14}$$

$$U_{rms} = a\,U_0^{\,b}\,d^{c}, \tag{15}$$

$$I = a\,U_0^{\,b}\,d^{c}. \tag{16}$$

The constants and the statistics are listed in Table 3. Figures 10a and 10b show the variations of U_{mean} and U_{rms} in zone C described by Equations 14 and 15, respectively.

The inlet jet momentum as an index to determine room flow characteristics has been used by many researchers (Gosman et al. 1980; Ogilvie and Barber 1989; Spitler et al. 1991). The dimensionless jet momentum number (J) is defined as $J = (QU_0)/(gV)$, where Q and U_0 are the ventilation flow rate and incoming jet air speed through the inlet, respectively; g is the acceleration of gravity; and V is the interior space volume. The floor velocities then were regressed to the jet momentum number at the inlet,

$$U_{mean} = \alpha J^{\beta}, \tag{17}$$

$$U_{rms} = \alpha J^{\beta}, \tag{18}$$

and are shown in Figure 11, where $J = (dlU_0^2)/(gLWH) = (dU_0^2)/(gLH)$, since the slot length, l, equals the room width, W, for this study; α and β are in Table 4.

The experimental data and the prediction from the above regression equations were compared. Data were randomly scattered around the prediction lines. The residuals were not significant by a test of the lack of fit, indicating an appropriate selection of the model.

The analysis of variance using the ANOVA procedure (SAS 1988) showed that none of the replicate effects was significant at the 5% level. However, the U_{mean} and U_{rms} at the floor were significantly different at the 5% level for 15 ach and at the 1% level for 40 ach for different combinations of inlet velocities and inlet slot heights. More

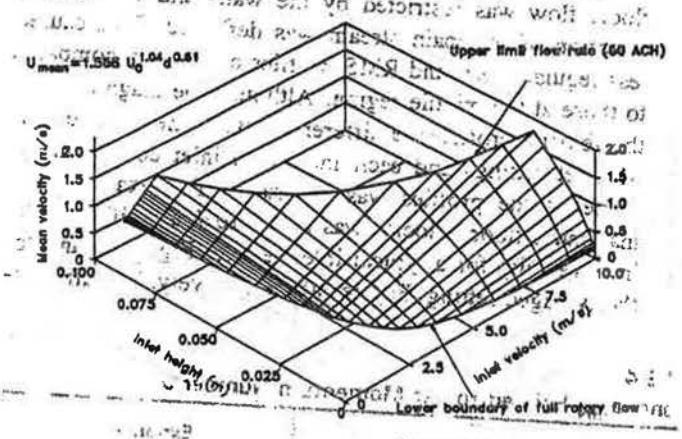

Figure 10a The response surface of mean velocity at the floor as a function of inlet velocity and inlet height in the full rotary flow zone.

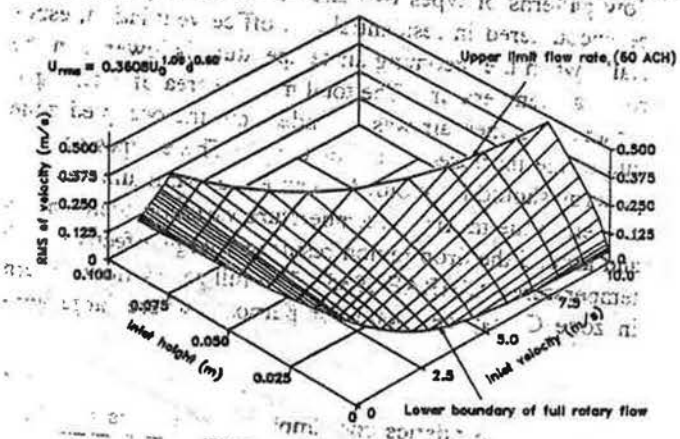

Figure 10b The response surface of the RMS value of velocity at the floor as a function of inlet velocity and inlet height in the full rotary flow zone.

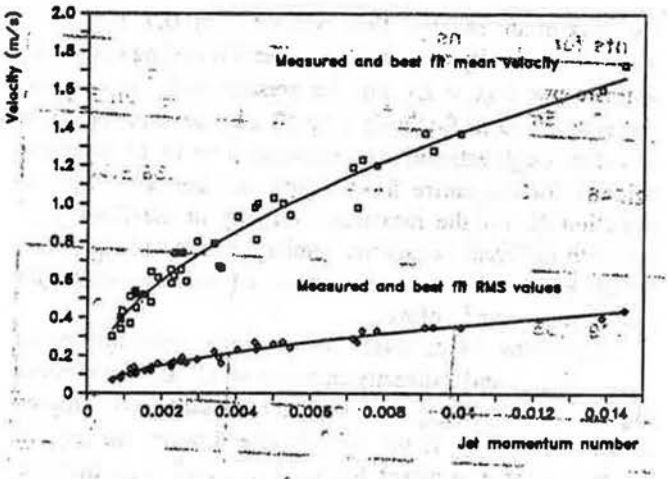

Figure 11 Actual and fitted mean velocity and RMS value at the floor correlated with the inlet-jet momentum number.

information about analysis of variance may be obtained from Jin (1991).

DISCUSSION

The type one flow pattern observed was similar to those where inlets are mounted in or near the ceiling, i.e., a high sidewall outlet, and the air is discharged horizontally as generalized by ASHRAE (1985). Velocity was stagnant, or normally less than 0.1 m/s (20 fpm), in the occupied zone. At the top of the room, air was entrained by the primary jet stream coming from the diffuser. The area and strength of entrainment were functions of incoming jet speed and inlet slot height. The combinations of the two inlet parameters that result in stagnant flow patterns in the occupied region were identified by the upper boundary of the stagnant zone A (Figure 7).

The intermediate zone was narrow, which includes the flow patterns of types two and three. These patterns may be encountered in residential and office ventilation, especially when the incoming air temperature is lower than the room air temperature. The total mixture area of discharged air and entrained air was extended into the occupied zone due to the increased throw of the jet. These types of flow patterns should be avoided because the maximum velocity as well as the maximum temperature variation occurring in and around the drop region result in a large effective draft temperature (ASHRAE 1985). The full rotary flow pattern in zone C may be useful for purposes where large ventilation rates are required, such as for night purging and industrial and agricultural ventilation.

Referring to the airflow rate plan (Figure 7), the boundaries at small inlet heights are much more sensitive to changes of inlet height, and a higher inlet velocity is needed to reach full rotary flow. At moderate to large inlet heights, the boundaries are nearly independent of the inlet height and full rotary flow may be achieved at less than 2 m/s (400 fpm) of inlet velocity. This is consistent with the theory of momentum transfer since the flow jet momentum at the inlet for the two examples is about the same. It is also implied that both inlet height and inlet velocity are important in determining the flow patterns at small inlet heights, and only inlet velocity is the determinant of flow pattern when the inlet height is greater than 40 mm (1.6 in.).

However, the regression lines show a greater deviation from the measured points at high inlet velocities and small inlet heights due to lack of information at those inlet settings. This results in the two lines crossing each other and a poor fit of data for inlet velocities greater than 4 m/s (800 fpm). Although the airflow rate plan was established from the data in this particular ventilation system and room dimensions, the principle is applicable to other types of ventilation systems and building geometries.

The normalized and averaged time-mean velocity and RMS value at five horizontal positions along the floor (Figures 8a and 8b) show the overall view of the velocity distribution. The mean air speed profiles at three middle positions approximated a wall jet distribution. The maximum velocity occurred at the location of 0.3 L from the wall opposite the inlet. Vertically, the speed increased to a maximum at about 0.1 m (4 in.) above the floor and then decreased, resembling a wall jet. A similar distribution was observed at the next two positions (0.5 L and 0.7 L) down the flow, but the magnitude at each corresponding point was smaller due to the loss of kinetic energy as the flow went on. At the corners or the intersection of wall and floor, flow was restricted by the walls and the velocity direction of the main stream was deflected. This caused less regular mean and RMS profiles of velocity compared to those at the middle region. Although the magnitudes of the velocity profiles are different between the average over 41 inlet settings and each individual inlet condition, the shape of the profiles was the same. For example, the maximum floor velocity was about 16% and 30% of the inlet velocity for a typical inlet setting (Figure 6) and for the averaged setting (Figure 8a), respectively. The differen-

TABLE 4
Statistics and Empirical Constants for U_{mean} and U_{rms} Related to Jet Momentum Number J

Dependent Variables	Equation Number	Standard Error	R^2	Intercept $\alpha \pm$ Std. Err.	Exponent $\beta \pm$ Std. Err.
U_{mean}	17	.071	.96	15.02 ± 1.38	.52 ± .02
U_{rms}	18	.018	.97	4.392 ± .394	.54 ± .02

ces in the shape between the two figures were negligible. This part of the work confirmed and furthered the observations of Baturin (1972), who only examined the velocity distribution to a limited distance from the inlet and along a wall, and those by Nielsen et al. (1978), who only measured the internal velocity at a few inlet configurations in a small model. The complete set of values for the 41 inlet combinations can be found in Jin (1991).

Measured and averaged mean and RMS values that represent the velocity characteristics in the entire floor region show a similar trend as affected by incoming jet speed and inlet slot height in zone C (Figures 9a and 9b). The largest values occurred at high inlet velocity, with the maximum at U_0 = 10 m/s (2,000 fpm) and d = 0.02 m (0.8 in.). The smallest values were associated with both low inlet speeds and inlet heights.

Dimensionless equations 9 and 12 regressed from the experimental data suggest that normalized floor mean velocity is almost independent of the Reynolds number either using L or d as the length scale. The asymptotic 95% confidence interval for constant b of the equations was (−0.026, +0.084). Therefore, when airflow was stable or fully rotary, the flow patterns as well as the normalized mean velocity were independent of Re_L or Re_d, which agreed well with the observation by Timmons et al. (1980) and Timmons (1984). However, the dimensionless terms were also proportional to the inlet height raised to a power of 0.58 for Equation 9 and 0.55 for Equation 12, for a constant L. This part of the result was not identified by them. An empirical exponent of 0.58 or 0.55 for (d/L) is very close to and consistent with the predicted result of a 0.50 power by Nielsen et al. (1978) and Gosman et al. (1980) for the maximum velocity in reverse flow.

The maximum velocity, U_x, in a plane wall jet at distance x from the supply opening may be expressed as (Nielsen 1989; ASHRAE 1985)

$$\frac{U_x}{U_0} = K_p\left(\frac{d}{x + x_0}\right)^{0.5} \qquad (19)$$

where

d = effective slot height,
U_0 = supply air velocity,
x_0 = additional distance to the virtual origin of the jet, and
K_p = empirical constant.

Nielsen (1989) expressed the maximum velocity in the reverse flow, U_{rm}, which is located close to the floor at a distance of (2/3) L from the supply opening, in a form similar to Equation 19,

$$\frac{U_{rm}}{U_0} = K_p\, K_{rm}\left(\frac{d}{L + x_0}\right)^{0.5} \qquad (20)$$

with an additional constant K_{rm} = 0.7 (Nielsen 1989). Comparing Equations 19 and 20, the $U_{rm} = K_{rm}U_L$, i.e., the maximum reverse flow velocity, is 0.7 times the maximum velocity of a wall jet under the ceiling extending to the sidewall ($x = L$). For the present study, $x_0 = 0$ and the exponent b in Equation 9 or 12 may be assumed to be zero for rough estimations. Equation 9 or 12 of the mean velocity for the entire floor region has the same form as Equation 20 for the maximum velocity in the floor level but with different constants. Similar results can be drawn for an RMS value from Equations 10 and 13, which has not been reported before.

Equations 14 through 16 gave the relationships of U_{mean}, U_{rms}, and I directly in terms of U_0 and d. Without big differences, U_{mean} and U_{rms} can be said to be proportional to ($U_0 d^{0.6}$). If the airflow rate through the inlet is maintained at a constant level, U_{mean} and U_{rms} increase with decreasing d and tend to vary with $d^{-0.4}$, very close to the predicted value of $d^{-0.5}$ by Nielsen et al. (1978) and Gosman et al. (1980).

Derived or regressed turbulence intensity seems unaffected by inlet configurations, since values of the exponents were very small. This can be seen from Figures 9a and 9b, in which the mean and RMS data increased or decreased correspondingly. Turbulence intensity is a ratio of RMS to mean velocity; therefore, it is relatively constant with the change of the inlet parameters.

U_{mean} and U_{rms} correlated well with J and were nearly proportional to the square root of J. These relationships not only agreed with the result of Spitler et al. (1991) for bulk air velocity but also provided further information regarding the flow turbulence, where bulk air velocity was defined as the average velocity measured at 896 points distributed throughout the room (Spitler et al. 1991). As further reported by Spitler et al., there is a linear relationship between the convective heat transfer coefficient (h) and the air mean velocity; the h in the occupied zone then can be obtained by $h = c_1 + c_2 J^{\beta}$, where c_1 and c_2 are empirical constants and β is listed in Table 4.

By analysis of variance, the U_{mean} and U_{rms} in the occupied zone were significantly different for the same ventilation rates due to the different combinations of incoming jet speed and inlet slot height. This analysis further indicates that the ventilation rate or Re_d cannot solely represent the floor velocity, since the same value causes different flow characteristics.

CONCLUSIONS

1. Airflow patterns in the floor region of a slot-ventilated room were divided into three zones on an airflow rate plan—the stagnant zone, the intermediate zone, and the fully rotary flow zone.
2. The boundaries dividing the three zones or types of flow patterns are expressed by the relation of (inlet width) (inlet velocity)^n = constant, where n is greater than 1.

3. The velocity in the occupied zone correlates with the inlet parameters very successfully as long as the room airflow patterns stay in the fully rotary zone. The floor velocity cannot be expressed solely by the ventilation rate through the inlet or the inlet Reynolds number but can be expressed by the jet momentum number. The nondimensional and dimensional floor velocity terms U_{mean}/U_0, U_{rms}/U_0, U_{mean}, and U_{rms} are all nonlinearly proportional to the inlet velocity as well as the inlet height, although U_{mean}/U_0 and U_{rms}/U_0 are very weakly correlated with Re_d or Re_L. Furthermore, U_{mean} and U_{rms} correlated well with J and are almost proportional to $J^{0.5}$.
4. Analysis of variance indicated that the same ventilation rates, due to the different combinations of inlet velocity and inlet slot height, resulted in significantly different reverse flow velocity in the occupied zone.

ACKNOWLEDGMENTS

This work was supported under Program 18 of the Ontario Ministry of Agriculture and Food/University of Guelph agreement. Support for Y. Jin was from the Canadian International Development Agency cooperative with Beijing Agricultural University, Beijing, PRC. Thanks are also given to P. Found, D.J. Gordon, E. Jordan, V. Pavlicik, and W. Verspagen for technical assistance.

REFERENCES

ASHRAE. 1985. *ASHRAE handbook—1985 fundamentals*, chapter 32. Atlanta: American Society of Heating, Refrigerating, and Air-Conditioning Engineers, Inc.

Baturin, V.V. 1972. *Fundamentals of industrial ventilation*. Oxford: Pergamon Press.

Chen, Q., A. Moser, and A. Huber. 1990. Prediction of buoyant, turbulent flow by a low-Reynolds-number k-ε model. *ASHRAE Transactions* 96(1): 546-573.

Gosman A.D., P.V. Nielsen, A. Restivo, and J.H. Whitelaw. 1980. The flow properties of rooms with small ventilation openings. *Transactions of the ASME, Journal of Fluids Engineering* 102: 316-323.

Hoff, S.J., K.A. Janni, and L.D. Jacobson. 1990. Modeling buoyant affected flow. ASAE Paper No. 90-4004. St. Joseph, MI: American Society of Agricultural Engineers.

Jin, Y. 1991. Airflow characteristics in a ventilated enclosure with a slot inlet opening. Ph.D. dissertation, School of Engineering, University of Guelph, Ontario.

Lam, C.K.G., and K.A. Bremherst. 1981. Modified form of the k-ε model for predicting wall turbulence. *Transactions of the ASME, Journal of Fluids Engineering* 103: 456-460.

Leigh, J.R. 1985. *Applied digital control theory: Design and implementation*. London: Prentice-Hall International Ltd.

Moog, W. 1981. Room flow tests in a reduced scale. *ASHRAE Transactions* 87(1): 1162-1180.

Nielsen, P.V. 1989. Numerical prediction of air distribution in room—Status and potentials. *Building Systems: Room Air and Air Contaminant Distribution*, pp. 31-38. Atlanta: American Society of Heating, Refrigerating, and Air-Conditioning Engineers, Inc.

Nielsen, P.V., A. Restivo, and J.H. Whitelaw. 1978. The velocity characteristics of ventilated rooms. *Transactions of the ASME, Journal of Fluids Engineering* 100: 291-298.

Ogilvie, J.R., and E.M. Barber. 1989. Jet momentum number: An index of air velocity at floor level. *Building Systems: Room Air and Air Contaminant Distribution*, pp. 211-214. Atlanta: American Society of Heating, Refrigerating, and Air-Conditioning Engineers, Inc.

Patel, V.C., W. Rodi, and G. Scheuerer. 1985. Turbulence models for near-wall and low Reynolds number flows: A review. *AIAA Journal* 23(9): 1308-1319.

SAS. 1988. *SAS/STAT user's guide*, release 6.03 ed. Gary, NC: SAS Institute Inc.

Spitler, J.D., C.O. Pedersen, and D.E. Fisher. 1991. Interior convective heat transfer in buildings with large ventilation flow rates. *ASHRAE Transactions* 97(1).

Timmons, M.B. 1984. Use of physical models to predict the fluid motion in slot-ventilated livestock structures. *Transactions of the ASAE* 27: 502-507.

Timmons, M.B., L.D. Albright, R.B. Furry, and K.E. Torrance. 1980. Experimental and numerical study of air movement in slot-ventilated enclosures. *ASHRAE Transactions* 86(1): 221-239.

Zhang, J.S., L.L. Christianson, and G.L. Riskowski. 1990. Regional airflow characteristics in a mechanically ventilated room under nonisothermal conditions. *ASHRAE Transactions* 96(1): 751-759.